Acid-Catalyzed Hydrolysis of 2-Methylene-1,3-dithiolane. Complete Analysis of a Three-Stage Reaction Mechanism

Tadashi Okuyama[1]

Contribution from the Faculty of Engineering Science, Osaka University, Toyonaka, Osaka 560, Japan, and the Department of Chemistry, University of Toronto, Toronto, Ontario M5S 1A1, Canada. *Received April 20, 1984*

Abstract: Hydrolysis of 2-methylene-1,3-dithiolane (**1**) consists of three reversible, consecutive reactions, involving 2-methyl-1,3-dithiolan-2-ylium ion (**2**) and 2-hydroxy-2-methyl-1,3-dithiolane (**3**) as intermediates. Kinetic examinations of reactions of **1** as well as the isolated salts of **2** and the product *S*-(2-mercaptoethyl) thioacetate (**4**) provided the rate constants for all the six individual steps of the hydrolysis. Above pH 3, the first protonation of **1** is mainly rate determining at limiting zero buffer concentration but the second hydration of **2** becomes progressively rate determining with increasing buffer concentration. Below pH 2, the third decay of the hydrogen ortho thioester **3** is the slowest step. In strong acid ($H_0 < -1.5$), the reverse of the last step, cyclization of **4**, becomes appreciable.

We recently discovered that ketene dithioacetals undergo acid-catalyzed hydrolysis through a mechanism involving a (partially) reversible protonation of the carbon–carbon double bond (eq 1).[2-5] Although similar reversibility has been found also in

$$RCH{=}C(SR')_2 + H_3O^+ \rightleftharpoons RCH_2C^+(SR')_2 + H_2O \overset{-H^+}{\rightleftharpoons} RCH_2C(OH)(SR')_2 \rightarrow RCH_2COSR' + R'SH \quad (1)$$

the hydrolysis of some enamines[6] and vinyl selenides,[7] this is in marked contrast to the closely related hydrolyses of ketene acetals,[8] vinyl ethers,[9] and vinyl sulfides,[10] all of which take place through rate-determining and nonreversible carbon protonation.

The present paper describes some kinetic results of the hydrolysis of a cyclic ketene dithioacetal, 2-methylene-1,3-dithiolane (**1**). In this case all three stages of the hydrolysis (eq 2–4) could

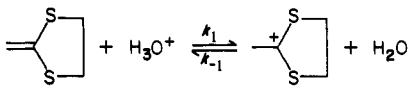

(2)

1 2

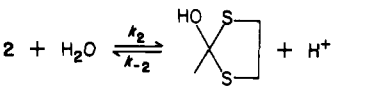

(3)

3

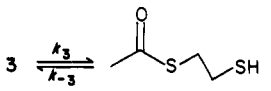

(4)

4

be monitored independently by means of UV spectrophotometry. The behavior of the intermediate carbocation **2** and the thiolester product **4** was also examined by using isolated samples of these materials, and a complete analysis of the kinetics of reactions 2–4 was therefore possible.

Results

The UV spectral changes of **1** in acid solutions show that the reaction is a multistep process. Although at pHs greater than 3 the decay of **1** (λ_{max} = 243 nm) occurs with simultaneous formation of the thiolester product **4** (λ_{max} = 233 nm) without the detectable appearance of any intermediate species, at higher acidities ([$HClO_4$] > 0.5 M) rapid generation of the carbocation **2** (λ_{max} = 330 nm) may be observed, and its slow decay to **4**, with an isosbestic point of λ = 235 nm, may be monitored. At intermediate pHs (0–2), the disappearance of **1** is much faster than the formation of the product **4** but no appreciable absorption attributable to **2** may be seen by conventional (slow) UV spectroscopy. This implies the existence of another intermediate which does not absorb UV light. A triphasic absorbance change in this pH region can in fact be observed by stopped-flow spectrophotometry: there is a rapid increase and then a biphasic decrease in absorbance at 330 nm. These spectral changes conform to the three-stage mechanism of reactions 2–4, which requires the hydrogen ortho thioester **3**, as well as the cation **2**, to be reaction intermediates. In concentrated acid, formation of cation **2** from thiolester **4** was also observed. Thus, decay of **1**, formation and decay of **2**, and formation of **4** can be monitored independently at 250, 330, and 233 nm, respectively.

Pseudo-first-order rate constants k_{obsd} for the disappearance of **1** (250 nm) at 25.0 ± 0.1 °C were obtained in aqueous solutions containing 0.5–1 vol % of CH_3CN at an ionic strength of 0.50 M, maintained with added KCl, by means of stopped-flow and conventional UV methods. The rate constants are proportional to acid concentration in dilute HCl solutions (0.001–0.01 M):[11] k_{HCl} = 130.1 M^{-1} s^{-1}. Data are given in Table S1 (supplementary material).

The appearance of **4** (233 nm) is slow below pH 2 (the rate is less than 10% that of the other reactions) and obeys pseudo-first-order kinetics.[12] The rate constants obtained are summarized in Table S1 and are shown plotted logarithmically against pH (H_0)

(1) Address correspondence at Osaka University. Fellowship from the Japan Society for the Promotion of Science and The Natural Sciences and Engineering Council of Canada that enabled the author to undertake part of this work at Toronto in the summer of 1982 is gratefully acknowledged.

(2) Okuyama, T.; Fueno, T. *J. Am. Chem. Soc.* **1980**, *102*, 6590–6591; **1983**, *105*, 4390–4395.

(3) Okuyama, T.; Kawao, S.; Fueno, T. *J. Am. Chem. Soc.* **1983**, *105*, 3220–3226.

(4) Okuyama, T.; Kawao, S.; Fueno, T. *J. Org. Chem.* **1984**, *49*, 85–88.

(5) Okuyama, T.; Kawao, S.; Fujiwara, W.; Fueno, T. *J. Org. Chem.* **1984**, *49*, 89–93.

(6) (a) Maas, W.; Janssen, M. J.; Stamhuis, E. J.; Wynberg, H. *J. Org. Chem.* **1967**, *32*, 1111–1115. (b) Coward, J. K.; Bruice, T. C. *J. Am. Chem. Soc.* **1969**, *91*, 5329–5339. (c) Sollenberger, P. Y.; Martin, R. B. *Ibid.* **1970**, *92*, 4261–4270.

(7) Hevesi, L.; Piquard, J. L.; Wautier, H. *J. Am. Chem. Soc.* **1981**, *103*, 870–875. Wautier, H.; Desauvage, S.; Hevesi, L. *J. Chem. Soc., Chem. Commun.* **1981**, 738–739.

(8) (a) Kankaanperä, A.; Tuominen, H. *Suom. Kemistil. B* **1967**, *40*, 271–276. (b) Gold, V.; Waterman, D. C. A. *J. Chem. Soc. B* **1968**, 839–849, 849–855. (c) Kankaanperä, A.; Aaltonen, R. *Acta Chem. Scand.* **1972**, *26*, 1698–1706. (d) Okuyama, T.; Kawao, S.; Fueno, T. *J. Org. Chem.* **1981**, *46*, 4372–4375. (e) Kresge, A. J.; Straub, T. S. *J. Am. Chem. Soc.* **1983**, *105*, 3957–3961.

(9) Salomaa, P.; Kankaanperä, A.; Lajunene, M. *Acta Chem. Scand.* **1966**, *20*, 1790–1801. Kresge, A. J.; Chiang, Y. *J. Chem. Soc. B* **1967**, 63–57, 58–61. Okuyama, T.; Fueno, T.; Nakatsuji, H.; Furukawa, J. *J. Am. Chem. Soc.* **1967**, *89*, 5826–5831.

(10) Okuyama, T.; Nakada, M.; Fueno, T. *Tetrahedron* **1976**, *32*, 2249–2252. Okuyama, T.; Masago, M.; Nakada, M.; Fueno, T. *Ibid.* **1977**, *33*, 2379–2381. McClelland, R. A. *Can. J. Chem.* **1977**, *55*, 548–551.

(11) Rate constants obtained at somewhat higher acidities ([$HClO_4$] < 1.14 M) are also roughly proportional to the acidity.

(12) Rate constants at pH 2 and 2.3 were obtained from the later part of the first-order plots.

0002-7863/84/1506-7134$01.50/0

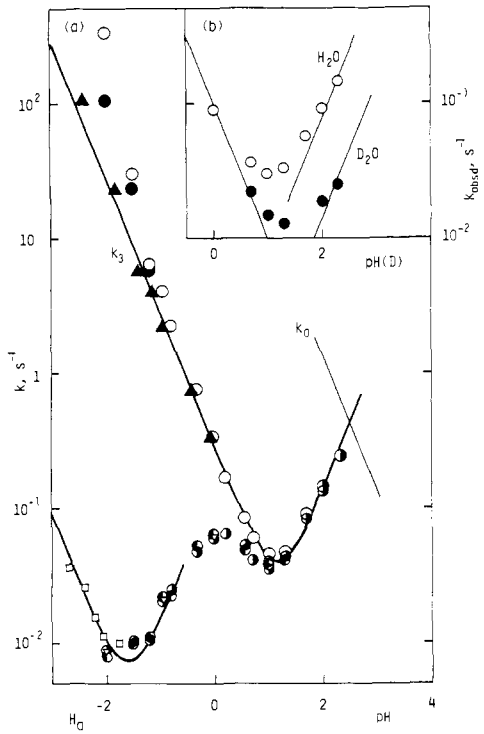

Figure 1. Dependences of observed (k_{obsd}) and calculated (k_3) rate constants on the acidities. (a) k_{obsd} were determined at 233 (◑) and 330 nm (◐) starting with **1** and at 330 nm (▽) starting with **2**. k_{obsd} for the formation of **2** from **4** were obtained at 330 nm (□). For the calculation of k_3 (○) and the corrections for the reverse reaction (●), see text. k_3 is plotted also against H_S (▲). (b) Rate constants obtained in H_2O (○) and in D_2O (●) are plotted against -log [HCl(DCl)].

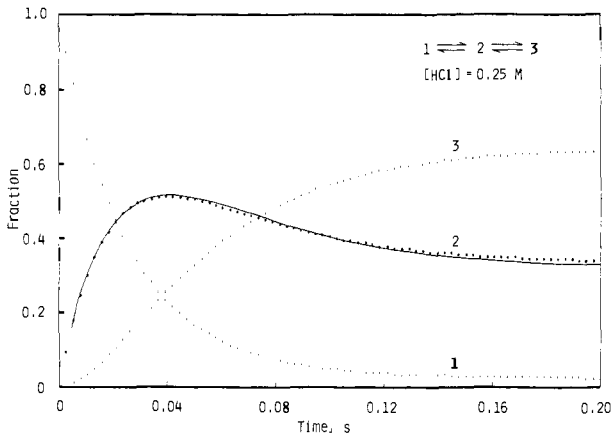

Figure 2. The initial part of the triphasic absorbance change at 330 nm in the reaction of **1** at [HCl] = 0.25 M. The dotted curves are theoretical ones with the rate constants given in Table III.

in Figure 1. The profile is complicated and has a maximum near pH 0.

Time-dependent absorbance changes at 330 nm, as observed by stopped-flow spectrophotometry, are triphasic in nature in the pH range 0–2 (Figure 2). The third stage is slow enough to be analyzed independently and gives pseudo-first-order kinetics. The rate constants so obtained are essentially identical with those provided by the increase in the 233-nm absorbance (see Figure 1 and Table S1). At still higher acidities, appearance of the 330-nm absorption is too rapid to follow ($<10^{-3}$ s), but the ensuing decay, which corresponds to the third stage of the mechanism of eq 2–4, can be followed easily by conventional UV method. The rate constants so obtained are similar to those measured at 233 nm. The decay of **2** could also be examined by starting with preformed salts of **2** and this method also gave similar constants in this acidity region (Figure 1 and Table S1).

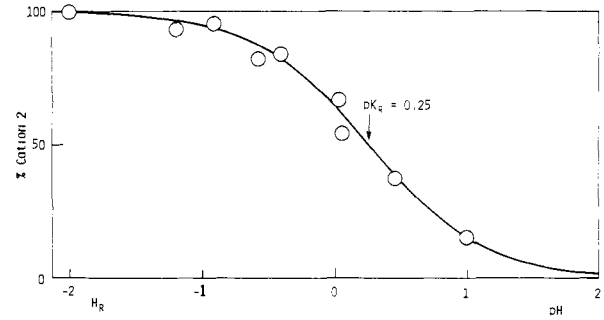

Figure 3. Plot of equilibrium fractions of **2** against H_R (pH). The curve is sigmoid with pK_R = 0.25.

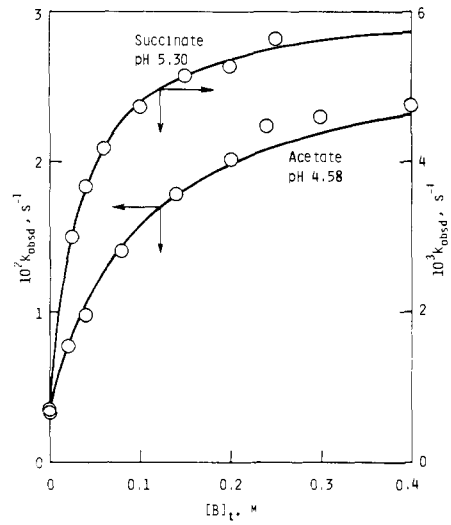

Figure 4. Buffer effects on the hydrolysis rate of **1** in the buffer solutions indicated. Curves are calculated by eq 7 with parameters given in Table I.

The first two stages of the triphasic change in the 330-nm absorbance correspond to the reactions of eq 2 and 3 and can be analyzed as a series of reversible reactions (eq 5). Solution of

$$\mathbf{1} \underset{k_{-1}}{\overset{k_1[H^+]}{\rightleftharpoons}} \mathbf{2} \underset{k_{-2}[H^+]}{\overset{k_2}{\rightleftharpoons}} \mathbf{3} \qquad (5)$$

$$[\mathbf{2}] = A_0 + A_1 \exp(-\lambda_1 t) + A_2 \exp(-\lambda_2 t) \qquad (6)$$

this kinetic scheme by a standard method[13,14] gives a complicated expression of the form of eq 6. The fitting of experimental data to this expression is facilitated by the fact that one rate constant (k_1) and two relationships among all four rate constants can be obtained independently from other experiments (see below).

Since the decay of **3** to **4** is slow at pH <2, equilibrium 5 is established before appreciable decay of **3** occurs. We could determine the equilibrium fraction of **2** from the 330-nm absorbance at the end of the first two stages of the triphasic change. The fraction of **2** varies sigmoidally with acidity, and analysis using the H_R acidity function[15,16] (Figure 3) gives pK_R = 0.25. Attempts to determine this equilibrium by a conventional UV method were unsuccessful probably owing to some mixing problems (the reaction is too rapid).

Deuterium solvent isotope effects were determined in HCl (DCl) solutions without any added salt (μ = [HCl(DCl)]). Rate constants for the disappearance of **1** (250 nm) were measured at [HCl(DCl)] $\simeq 10^{-3}$ M (Table S2, supplementary material): k_{HCl} = 97.18 ± 1.74 M^{-1} s^{-1}, k_{DCl} = 31.77 ± 0.29 M^{-1} s^{-1}, k_{HCl}/k_{DCl} = 3.06 ± 0.09. Rate constants for the formation of **4** (233 nm)

(13) Szabó, Z. G. "Comprehensive Chemical Kinetics"; Bamford, C. H., Tipper, C. F. H., Eds.; Elsevier: Amsterdam, 1969; Vol. 2, pp 29–31.
(14) Moore, J. W.; Pearson, R. G. "Kinetics and Mechanism", 3rd ed.; Wiley: New York, 1981; pp 296–300.

Table I. Buffer Effects on the Hydrolysis Rate of **1**[a]

buffer	pH[b]	10^3k_0,[c] s^{-1}	$10^3\Delta k_{max}$,[d] s^{-1}	K_{app},[d] M	k_2/k_{-1}[e]
formate	3.57[f]	35.0	183 (27)	0.178 (0.036)	5.23
	4.18	8.60	57.2 (1.9)	0.153 (0.007)	6.65
acetate	3.98	13.62	73.8 (3.1)	0.164 (0.011)	5.42
	4.58	3.42	24.3 (2.3)	0.096 (0.014)	7.11
	4.97	1.39	12.2 (0.4)	0.079 (0.004)	8.78
	5.18	0.860	6.45 (0.14)	0.076 (0.003)	7.50
	5.23	0.766	5.97 (0.19)	0.063 (0.004)	7.79
succinate	5.30	0.652	5.51 (0.07)	0.033 (0.001)	8.45
	5.75	0.231	1.96 (0.06)	0.028 (0.002)	8.48

[a] Ionic strength 0.50 M (KCl), 25 °C. [b] ±0.01 unless otherwise noted. [c] Calculated as $k_0 = 130.1\ [H^+]\ s^{-1}$. [d] Standard deviations are given in parentheses. [e] $\Delta k_{max}/k_0$. [f] ±0.02.

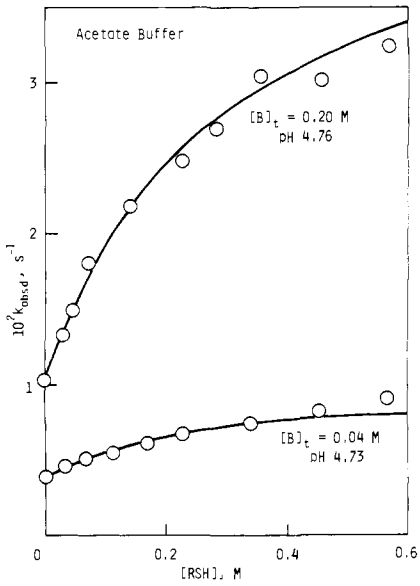

Figure 5. Effects of 2-mercaptoethanol (RSH) on the hydrolysis rate of **1** in acetate buffer solutions of (a) $[B]_t = 0.04$ M and pH 4.73 and (b) $[B]_t = 0.20$ M and pH 4.76. Curves are calculated by the equations (a) $10^3k_{obsd} = 3.89 + 6.01[RSH]/(0.256 + [RSH])$ and (b) $10^2k_{obsd} = 1.024 + 3.55[RSH]/(0.294 + [RSH])$.

were also determined at [HCl] = 0.005–1 M and [DCl] = 0.005–0.2 M and are shown plotted against pH(D) in Figure 1b. The data are listed in Table S2.

Rates of disappearance of **1** (250 nm) were measured in carboxylate buffer solutions over the pH range 3.5–5.7. The observed rate constants are summarized in Table S3 (supplementary material). They increase with buffer concentration $[B]_t$, following a saturation curve (Figure 4), as observed before with other ketene dithioacetals.[2-5] These curves can be described by eq 7, where

$$\Delta k = \Delta k_{max}[B]_t/(K_{app} + [B]) \quad (7)$$

$\Delta k = k_{obsd} - k_0$ and $\Delta k_{max} = k_{max} - k_0$. The interpretations of the limiting rate constants k_0 and k_{max}, which refer to zero and infinite buffer concentrations, respectively, and the parameter K_{app} in terms of individual step rate constants are given below under Discussion. Values of k_0 were supplied from experiments performed in dilute HCl solutions, and Δk_{max} and K_{app} were evaluated by least-squares analysis of plots of $1/\Delta k$ vs. $1/[B]_t$; the results are summarized in Table I.

The effect of added 2-mercaptoethanol (RSH) on the rate of disappearance of **1** (250–260 nm) was examined while keeping the total organic component (CH_3CN + RSH) of the reaction solutions constant at 10 or 5 vol %. Observed rate constants obtained in this way are given in Table S3. In HCl solutions ([HCl] ≃ 0.05 M), the rate was hardly affected by added thiol ([RSH] < 0.284 M). In acetate buffer solutions of pH 4.7 ($[B]_t$ = 0.04 and 0.20 M), however, the rate increased markedly with thiol concentration and followed a saturation curve expressed by a relationship similar to eq 7[3-5] (Figure 5).

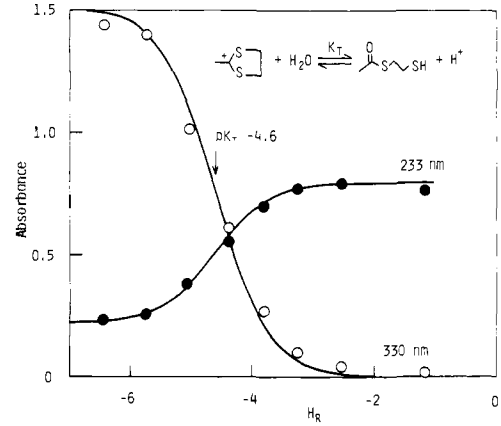

Figure 6. Plots of equilibrium absorbances at 330 (○) and 233 nm (●) against H_R for the reaction **2** ⇌ **4**. Curves are sigmoid with $pK_T = -4.6$.

Table II. Rates of the Decay of Cation **2** in Aquous Acetonitrile Solutions[a]

conditions	k_{obsd}, s^{-1}
[HCl] = 0.001–0.25 M	55.2 ± 1.7
unbuffered water	55.5
chloroacetate (1.0)[b]	(60 ± 6) + (714 ± 79)$[B]_t$
formate (1.0)[b]	(68 ± 3) + (835 ± 43)$[B]_t$
acetate (4.0)[b]	(42 ± 5) + (1290 ± 70)$[B]_t$
acetate (1.0)[b]	(30 ± 24) + (3940 ± 480)$[B]_t$

[a] Measured by the stopped-flow method in 1:1 (v/v) CH_3CN–H_2O (μ = 0.25) at 25 °C. [b] Buffer ratios are given in parentheses.

When thiolester **4** is dissolved in concentrated $HClO_4$ solutions, an absorption at 330 nm gradually develops. This change is interpreted as the reverse of reactions of eq 3 and 4. Rates for the formation of **2** from **4** were measured at $[HClO_4]$ = 4–5.8 M, and values of k_{obsd} are shown plotted against the H_0 acidity function[15,16] in Figure 1. Equilibrium absorbances were also determined, both at 330 (**2**) and at 233 nm (**4**). The absorbance at 330 nm increased while that at 233 nm decreased with acidity, as required by eq 8, and both changes followed sigmoid curves

$$2 + H_2O \overset{K_T}{\rightleftharpoons} 4 + H^+ \quad (8)$$

when plotted against the H_R function (Figure 6) and gave pK_T = −4.6. Similar equilibrium absorbances were also obtained by starting with salts of **2**.

The reaction of preformed salts of **2** was examined with stopped-flow techniques by mixing an acetonitrile solution of **2** with aqueous HCl or buffer solutions (μ = 0.50 M); the resulting reaction media were then 1:1 (v/v) CH_3CN–H_2O with an ionic strength of 0.25 M. Rates of disappearance of **2** were measured at 330 nm. The results are summarized in Table II, and values of k_{obsd} are given in Table S4 (supplementary material). The rate constants obtained in dilute HCl solutions ([HCl] < 0.25 M) were essentially constant, k_{obsd} = 55.2 ± 1.7 s^{-1}. In more acidic solutions, k_{obsd} decreased rapidly with acidity. The rate in 1:1 CH_3CN–H_2O solutions without any added salt (i.e., zero ionic strength) was slightly less ($k_{obsd} \simeq 51\ s^{-1}$) than that at higher ionic strengths. Rates were strongly buffer dependent and increased linearly with buffer concentrations in carboxylate buffer solutions. The slopes increase with basicity of the buffer and appear to reflect general-base catalysis of the reaction. Rate constants extrapolated to zero buffer concentration agree with those obtained in dilute HCl solutions, though the experimental uncertainties are relatively large.

Discussion

The process investigated here involves three consecutive, reversible reaction steps (eq 2–4), and the kinetics are therefore of

(15) Rochester, C. H. "Acidity Functions"; Academic Press: London and New York, 1970.
(16) Kresge, A. J.; Chen, H. J.; Capen, G. L.; Powell, M. F. *Can. J. Chem.* **1983**, *61*, 249–256.

necessity quite complicated. However, some simplifications are possible under certain reaction conditions. Below pH 2 the last step (eq 4) of the three-stage hydrolysis is much slower than the first two (eq 2 and 3), and independent analyses of the kinetics of the rapid and slow reactions are possible. Above pH 3, on the other hand, step 3 becomes very rapid and step 1 or 2 is rate determining. The reverse of the last step (k_{-3}) is appreciable only in very strong acid.

pH above 3. At higher pH the process may be analyzed by the reaction sequence of eq 9. The value of $k_{-2}[H^+]$ is so small in

$$\mathbf{1} \underset{k_{-1}'[B]}{\overset{k_1[H^+]}{\underset{k_1'[BH^+]}{\rightleftharpoons}}} \mathbf{2} \xrightarrow{k_2} \mathbf{3} \xrightarrow{\text{rapid}} \mathbf{4} \qquad (9)$$

$$k_0 = k_{HCl}[H^+] = k_1k_2[H^+]/(k_{-1} + k_2) \qquad (10)$$

this pH region that k_0 (in the absence of buffer) can be described by eq 10, which results from application of the steady-state approximation to **2**.[17] In buffer solutions a curved dependence of observed rate constant on buffer concentration occurs because only the first step is catalyzed by buffer,[18] and the rate-determining step changes with buffer concentration.[2-5] Thus, the limiting rate constant k_{max} is attained when the second step becomes rate determining with the first step in rapid equilibrium (eq 11). It

$$k_{max} = k_1k_2[H^+]/k_{-1} \qquad (11)$$

follows that k_{max} should be proportional to acid concentration, and this is approximately the case with $k_1k_2/k_{-1} = 1080 \pm 200$ M^{-1} s^{-1}. The parameter K_{app} of eq 7 is equal to the buffer concentration at which half the maximum rate increase is attained; it is described by eq 12, where k_{-1}' is the catalytic constant for

$$K_{app} = (k_{-1} + k_2)/k_{-1}'\alpha \qquad (12)$$

the deprotonation of **2** by a general base and $\alpha = [B]/[B]_t$. In accord with eq 12, values of K_{app} decrease with the basicity of the buffer (Table I).

The rate constant ratio k_2/k_{-1} can be calculated by eq 13, which

$$\Delta k_{max}/k_0 = k_2/k_{-1} \qquad (13)$$

is derived from eq 10 and 11; values are given in the last column of Table I. Although these vary somewhat with pH, the average is $k_2/k_{-1} = 7.24 \pm 1.30$. That is, the initial protonation step is largely rate determining in the absence of buffer, but the second step, hydration of the carbocation **2**, becomes progressively rate determining in buffer solutions as the buffer concentration increases.

This analysis is supported by the effects of added thiol on the rate of disappearance of **1**. Thiols are good nucleophiles even in acid solution and can compete effectively with water in wholly aqueous solutions.[2-5] If a nucleophilic reaction of water is involved in the rate-determining step, added thiol should accelerate the overall reaction, but otherwise no effects of the thiol should be observed. In the present reactions, 2-mercaptoethanol had negligibly small effects in HCl solutions,[19] but accelerative effects were clearly observed in acetate buffer solutions (Figure 5). The effects are stronger at higher concentrations of the buffer. These observations agree completely with those expected from the results of buffer experiments. The accelerative effects of the thiol level off at higher thiol concentrations, as anticipated, because the first step becomes rate determining as the second step is accelerated.

Deuterium solvent isotope effects on the rate of disappearance of **1** were determined in HCl (DCl) solutions at pH ca. 3. The result, $k_{HCl}/k_{DCl} = 3.06$, conforms to a mechanism involving mostly rate-determining protonation of the double bond. The magnitude of this isotope effect is similar to that observed for vinyl ether hydrolysis.[20]

pH Range 0-2. In the pH range 0-2, the last step of the reactions is very slow, and the first two steps can be analyzed independently as a sequence of reversible reactions (eq 5). The equilibrium concentration of **2** under these conditions could be determined by the stopped-flow method. The sigmoid H_R dependence shown in Figure 3 is described by eq 14, with the relationship of eq 15, and gives $pK_R = 0.25$.

$$\text{fraction } \mathbf{2} = h_R/(K_R + h_R) \qquad (14)$$

$$K_R = (k_{-1}/k_1) + (k_2/k_{-2}) = 0.56 \qquad (15)$$

Integration of the kinetic equations for the reaction scheme of eq 5 leads to a complicated expression of the form of eq 6,[13,14] from which it is difficult to evaluate the four rate constants of the scheme. In the present case, however, k_1 and the ratio k_2/k_{-1} are already known, and the relationship of eq 15 is also available. With these constraints, we were able to use eq 6 to evaluate all four rate constants by adjusting the three constants (k_{-1}, k_2, and k_{-2}) until a good fit to the experimental stopped-flow traces was obtained. Such calculations were done for data obtained at [HCl] = 0.10 and 0.25 M. The same set of constants were obtained and these constants reproduced reasonably the data at [HCl] = 0.025 and 0.50 M. A typical fit is shown in Figure 3 and all of the results are summarized in Table III; we estimate that these rate constants are accurate to better than ±10%.

Table III. Kinetic Parameters[a]

k_{HCl}, M^{-1} s^{-1}	130.1[b]
k_1, M^{-1} s^{-1}	148
k_{-1}, s^{-1}	2.9
k_2, s^{-1}	21
k_{-2}, M^{-1} s^{-1}	39
k_3^A, M^{-1} s^{-1}	0.28
k_3^B, M s^{-1}	1.4×10^{-3}
k_{-3}, M^{-1} s^{-1}	9×10^{-5}
pK_R	0.25
pK_T	-4.6

[a] 25 °C in aqueous solutions. [b] 137 M^{-1} s^{-1} in 10 vol % CH_3CN-H_2O (μ = 0.45 M) at 30 °C.

We were able in this way to determine separately the two equilibrium constants, $K_1(=k_1/k_{-1}) = 51$ M^{-1} and $K_2(=k_2/k_2) = 0.54$ M, for the protonation of **1** and the hydration of **2**. This shows that the main contribution to the apparent constant K_R comes from the second equilibrium (K_2); the overall equilibrium therefore conforms to the H_R function as observed (eq 14). The magnitudes of K_1 and K_2 imply that the equilibrium concentration of the olefinic substrate **1** is equal to that of the carbocation **2** at pH 1.7, and **2** and its hydrate **3** exist in the same concentration at pH 0.27.

Successful determinations of the equilibrium constants for the protonation of olefins to give carbocations are rare. The only example we are aware of is the equilibrium between an enamine and an iminium ion (eq 16).[6c] Because of the stability of the

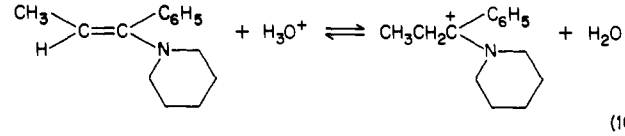

(16)

iminium ion the equilibrium constant is very large (log K_I = 9.76).[6c] More information on the hydration equilibria of carbocations is available, and this seems to indicate that oxo carbocations

(17) Equation 10 holds at pH's down to 2 and k_{HCl} is determined from k_{obsd} for the disappearance of **1** at [HCl] = 0.001-0.01 M.

(18) (a) Hydration of a stable carbocation, 2-aryl-1,3-dithiolan-2-ylium ion, was found to be catalyzed by general bases,[18b] but general catalysis of the hydration of the less stable cation **2** may be negligibly weak.[2-5] (b) Okuyama, T.; Fujiwara, W.; Fueno, T. *J. Am. Chem. Soc.* **1984**, *106*, 657-662.

(19) The maximum rate increase induced by added thiol and the thiol concentration when a half the maximum rate increase is attained are described by $\Delta k_{max}^T = (k_{-1}/k_2)k_0$ and $K_{app}^T = (k_{-1} + k_2)/k_t$, respectively, where k_t is the rate constant for the reaction of RSH with **2**.[3] Furthermore, k_2/k_t was found to be about 1 M at pH <2 for 1,1-bis(methylthio)-2-phenylethene.[2] Thus, $\Delta k_{max}^T = 0.14k_0$ and $K_{app}^T = 1$ M can be estimated for the present reaction. The estimated rate increase induced by 0.284 M of RSH used here is only about 3% of the rate observed in the absence of RSH.

(20) Kresge, A. J.; Sagatys, D. S.; Chen, H. L. *J. Am. Chem. Soc.* **1977**, *99*, 7228-7233.

are less stable than their sulfur analogues; for example, the pK_R of the phenyl derivative **5** has been estimated to be about −0.6,[21]

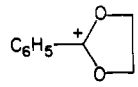

5

which is some 2.5 pK units lower than that for the sulfur analogue.[18b]

Rate constants for the decay of cation **2** in aqueous solution, $k_2 = 21\ s^{-1}$ and $k_{-1} = 2.9\ s^{-1}$, may be compared with those obtained in 1:1 CH_3CN–H_2O. In the latter medium, k_{obsd} ($=k_2 + k_{-1}$) = $55\ s^{-1}$ at [HCl] = 0–0.25 M. Since k_2/k_{-1} is large in this solvent, $k_2 \simeq 50\ s^{-1}$. The reduced stabilization of **2** in the less polar solvent must be responsible for the greater value of k_2. The decay of **2** is strongly buffer dependent in 1:1 CH_3CN–H_2O. This dependence must arise from the k_{-1} part of k_{obsd}, deprotonation of **2** by the buffer base (k_{-1}').

Formation of Thiolester 4. The formation of **4**, as monitored by the increase in the 233-nm absorbance, is slow enough below pH 2 to be analyzed independently. However, as may be seen in Figure 1, k_{obsd} changes in a complicated manner with acidity. Since the first two steps are in rapid equilibrium under these conditions, k_{obsd} must be proportional to the equilibrium fraction of the intermediate **3** (eq 17). By using values of K_1 and K_2

$$k_{obsd} = K_2k_3/((1/K_1) + K_2 + h_R) \qquad (17)$$

obtained above, we were able to calculate k_3 from k_{obsd}; the results are shown plotted against the H_0 acidity function in Figure 1. The acidity–rate profile is an inverse bell in shape; this shows that the decay of the hydrogen ortho thioester **3** is catalyzed both by acid and base. Positive deviations are, however, apparent at higher acidities. These deviations must reflect in part the contribution from the reverse reaction (k_{-3}). Points obtained after correction for this[22] (plotted with closed circles in Figure 1) still show considerable upward deviations. Another cause of such deviations could be a steeper acidity dependence for the sulfur protonation, as generally found for sulfides and thiols.[23] The acidity function H_S for sulfur protonation may be defined by eq 18, according to

$$H_S = 1.3H_0 + 0.3(\log\ [HX]) \qquad (18)$$

the results of Scorrano et al.[23] The rate constant k_3 nicely follows this acidity function as shown in Figure 1 with closed triangles. The profile is thus described by eq 19, where $k_3^A = 0.28\ M^{-1}\ s^{-1}$

$$k_3 = k_3^Ah_S + k_3^B/[H^+] \qquad (19)$$

and $k_3^B = 1.4 \times 10^{-3}\ M\ s^{-1}$. The acid-catalyzed decay of **3** must involve sulfur protonation as a rapid equilibrium.

Observed complication of the apparent $H_0 - \log k_{obsd}$ profile around $H_0 = 0$ arises from the difference in the dependences of the intermediate concentration and the rate on the acidity. The equilibrium concentration of **3** involving water activity is dependent on the H_R function, while the acid-catalyzed decay of **3** depends on the H_S function. These acidity functions show rapidly changing sensitivity against acid concentration in this range of acidity. If we use a wrong K_R value for the estimation of the equilibrium fraction of **3** (e.g., $K_R = -0.5$), the $H_0 - \log k_3$ profile becomes complicated with a plateau region around $H_0 = 0$, which seemed to suggest a complicated mechanism of the decay of **3**.[24]

Deuterium solvent isotope effect on the rates of formation of **4** may be seen in Figure 1b. There appears to be little isotope effect on the acid-catalyzed portion of this reaction, but the base-catalyzed reaction is considerably faster in H_2O than in D_2O. These results can be accommodated using the reaction mechanisms given in eq 20. It would seem reasonable to assume that the

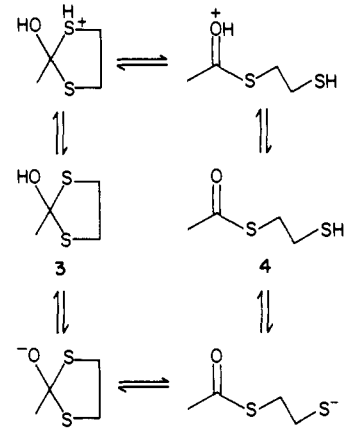

(20)

isotope effect in each case arises from the acid–base equilibria involved, that for protonation on sulfur for the acid-catalyzed path, and that for ionization of an O–H bond in the base-catalyzed route. It is well-known that oxygen acids are considerably weaker in D_2O than in H_2O, i.e.; $(K_a)_{H_2O}/(K_a)_{D_2O} > 1$, and the concentration of the reactive conjugate base of **3** will therefore be less in D_2O than in H_2O, leading to $(k_{obsd})_{H_2O}/(k_{obsd})_{D_2O} > 1$. Less is known about solvent isotope effects on the ionization of sulfur acids, but what information is available indicates that these effects are much weaker than those on oxygen acids, due primarily to the lower vibrational frequencies of S–H bonds. The isotope effect on the sulfur protonation equilibrium of the acid-catalyzed path might therefore be not very different from unity, and an overall isotope effect also not too different from unity might be expected. These isotope effects thus suggest that the proton-transfer steps of the mechanisms of eq 20 are rapid equilibria and that the ring openings are rate determining.

The formation of cation **2** from **4** was observed in strong acid. This process is reversible, and the equilibrium absorbances at 330 nm (**2**) as well as those at 233 nm (**4**), measured using either **2** or **4** as starting materials, fit sigmoid curves, as shown in Figure 6. Both curves give $pK_T = -4.6$. This equilibrium involves water (eq 7) and therefore conforms to H_R. The rate-determining step of the reaction **2** ⇌ **4** in this acidity region must be the interconversion of **3** and **4**, and the observed rate constant k_{obsd} should be the sum of the rate constants for the forward and reverse reactions of the complete reversible change. The overall rate constant for the formation of **4** decreases with acidity, in spite of acid catalysis of the decay of **3**, as mentioned above, and the reverse reaction (cyclization) is catalyzed by acid. As a result, the apparent profile in this acidity region is an inverse bell in shape, as may be seen in Figure 1. The acid-catalyzed portion of the inverse bell with H_0 gives $k_{-3} = 9 \times 10^{-5}\ M^{-1}\ s^{-1}$.

We can now calculate the equilibrium constant for reaction 4: K_{-3} for the cyclization of **4** to lead to **3** (the reverse of eq 4) is 3.2×10^{-4}, or $\Delta G° = 4.8$ kcal/mol. Hydroxydithiolane **3** closely resembles a tetrahedral intermediate involved in acyl-transfer reactions,[25,26] and the quantitative evaluation of the stability of this species may supplement the recent efforts of such determinations.[26-28] The above result may be compared with similar values for the oxygen analogues (eq 21).[29,30] Cyclization of the thioester to give the tetrahedral intermediate occurs more easily

(21) Ahmad, M.; Bergstrom, R. G.; Cashen, M. J.; Chiang, Y.; Kresge, A. J.; McClelland, R. A.; Powell, M. F. *J. Am. Chem. Soc.* **1979**, *101*, 2669–2677.

(22) Subtracted $k_{-3}h_0$ from the calculated values (see below).

(23) Bonvicini, P.; Levi, A.; Lucchini, V.; Scorrano, G. *J. Chem. Soc. Perkin Trans. 2* **1972**, *2267*–2269. Bonvicini, P.; Levi, A.; Lucchini, V.; Modena, G.; Scorrano, G. *J. Am. Chem. Soc.* **1973**, *95*, 5960–5964. Perdoncin, G.; Scorrano, G. *Ibid.* **1977**, *99*, 6983–6986.

(24) Such a suggestion was made for the results obtained during the hydrolysis of 2-methylene-1,3-dithiane,[5] but it is probably wrong. The estimated value of pK_R might have been too low.

(25) Capon, B.; Ghosh, A. K.; Grieve, D. McL. A. *Acc. Chem. Res.* **1981**, *14*, 306–312.

(26) McClelland, R. A.; Santry, L. J. *Acc. Chem. Res.* **1983**, *16*, 394–399.

(27) Guthrie, J. P. *Acc. Chem. Res.* **1983**, *16*, 122–129.

(28) Fastrez, J. *J. Am. Chem. Soc.* **1977**, *99*, 7004–7013.

(29) Guthrie, J. P. *Can. J. Chem.* **1977**, *55*, 3562–3574.

(30) McClelland, R. A.; Ahmad, M.; Bohonek, J.; Gedge, S. *Can. J. Chem.* **1979**, *57*, 1531–1540.

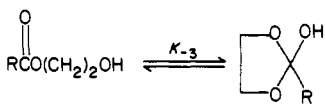

(21)

$R=CH_3$, $\Delta G°=10.7$ kcal/mol[29]
$R=C_6H_5$, $\Delta G°=11.8$ kcal/mol[30]

than that of the ester. This may arise from the facts that the ester linkage is more stabilized by the resonance than the thioester group[28,31] and that the (equilibrium) nucleophilicity of the thiol function is greater than that of the hydroxyl group.[28,32]

Thiolester **4** does not undergo hydrolysis to give acetic acid and 1,2-ethanedithiol even in very strongly acidic solution. This is not unexpected: a cyclization to give **3**, which is an intramolecular nucleophilic addition of the thiol to the protonated carbonyl group, occurs much more readily than the nucleophilic attack of water.

Reactivity. Finally, the reactivity of the cyclic ketene dithioacetal **1** may be compared with those of some related compounds. The rate of protonation of **1** (k_1) is 3–4 times greater than those of the acyclic and six-membered cyclic analogues, **6**[3] and **7**.[5] This

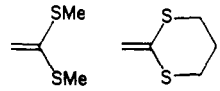

6 **7**

difference could arise from a greater conjugative stabilization of the transition state, resembling that in the product carbocation, due to the forced planarity of the five-membered ring. Similar but stronger effects appear in oxygen analogues; e.g., the acid-catalyzed hydrolysis of the ketene acetal **8**[8b] occurs 20 times faster than that of **9**.[8e]

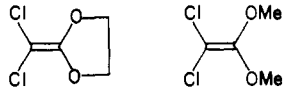

8 **9**

Experimental Section

Materials. 2-Methylene-1,3-dithiolane (**1**) and 2-methyl-1,3-dithiolan-2-ylium (**2**) perchlorate were prepared as described previously.[33] *S*-(2-Mercaptoethyl) thioacetate (**4**) was obtained by the reaction of 1,2-ethanedithiol with acetic anhydride in the presence of sodium acetate: bp 92 °C (17 mmHg). Other chemicals were obtained as before.[2,3]

Equilibrium and Kinetic Measurements. Reactions were carried out at 25.0 ± 0.1 °C in aqueous solutions containing 0.5–1.0 vol % of CH_3CN, and the ionic strength was adjusted at 0.50 M by adding KCl. Effects of thiol were examined in 10 vol % CH_3CN–H_2O at the ionic strength 0.45 M (KCl). Buffer solutions were prepared in the same way as before.[3] Reactions were monitored spectrophotometrically on Cary Model 118C and Durrum-Gibson stopped-flow spectrophotometers, and some additional runs were performed by using Shimadzu UV 200 and Union RA 1100 stopped-flow spectrophotometers. The reactions monitored by conventional UV spectrophotometry were started by introducing 15–30 μL of the stock solution of the substrate from a microsyringe into 3 mL of an aqueous solution thermally equilibrated in a stoppered cuvette. Rapid reactions carried out on stopped-flow apparatus were initiated by mixing a solution of **1** in very dilute NaOH (10^{-4}–10^{-3} M) with an equal volume of the appropriate aqueous acid. The reactions of **2** were performed by stopped-flow mixing of a solution of **2** in dry acetonitrile with an equal volume of appropriate aqueous solution.

Equilibrium absorbances were read after the reactions concerned had gone to completion. The disappearance of **1** was followed by the decrease in absorbance at 250 nm (or 260 nm for some runs with added thiol); these changes gave good pseudo-first-order kinetics. The appearance of **4** was monitored by the increase in absorbance at 233 nm. First-order plots for this change gave concave curvature at $[HClO_4(HCl)] = 0.5$–2 M, and values of k_{obsd} were therefore obtained from the initial part. The slower decrease in the 330-nm absorbance also showed similar curvature of first-order plots in this acidity range, but the rapid decrease in absorbance at 330 nm when **2** was the starting material followed first-order kinetics. The biphasic decrease of the triphasic absorbance change at 330 nm observed in the pH range 0–2 was analyzed as two independent first-order reactions. The initial parts of these curves were compared with theoretical ones calculated by using a Casio FP 1000 microcomputer with an appropriate set of rate constants.

The pH values of buffer solutions were measured on a Beckmann research pH meter. Values of the H_0 and H_R acidity functions were calculated from the polynominal expressions supplied in ref 16.

Acknowledgment. I thank Professor A. J. Kresge for his hospitality in Toronto, many enlightening discussions, and careful examination of the manuscript and Professor T. Fueno for helpful discussions.

Registry No. 1, 26728-22-3; **2**, 92220-33-2; **2**·ClO_4, 92220-34-3; **3**, 92220-35-4; **4**, 92220-36-5; 1,2-ethanedithiol, 540-63-6; 2-mercaptoethanol, 60-24-2; formate, 71-47-6; acetate, 71-50-1; succinate, 56-14-4; chloroacetate, 14526-03-5.

Supplementary Material Available: Tables S1–S3 of observed rate constants for the reaction of **1** and Table S4 of those for the reaction of **2** (5 pages). Ordering information is given on any current masthead page.

(31) Bruice, T. C.; Benkovic, S. "Bioorganic Mechanisms"; Benjamin: New York, 1966; Vol. 1, pp 266–268.
(32) Jencks, W. P. *Prog. Phys. Org. Chem.* **1964**, *2*, 63–128. Lienhard, G. E.; Jencks, W. P. *J. Am. Chem. Soc.* **1966**, *88*, 3982–3995.
(33) Okuyama, T. *Tetrahedron Lett.* **1982**, *23*, 2665–2666.